Multilevel DC Link Inverter for Brushless Permanent Magnet Motors with Very Low Inductance

Gui-Jia Su, *Senior Member*, *IEEE*, Donald J. Adams

Oak Ridge National Laboratory
National Transportation Research Center
Knoxville, Tennessee 37932
Email: sugj@ornl.gov

Abstract [*] **-Due to their long effective air gaps, permanent magnet motors tend to have low inductance. The use of ironless stator structure in present high power PM motors (several tens of kWs) reduces the inductance even further (<100μH). This low inductance imposes stringent current regulation demands for the inverter to obtain acceptable current ripple. An analysis of the current ripple for these low inductance brushless PM motors shows that a standard inverter with the most commonly used IGBT switching devices cannot meet the current regulation demands and will produce unacceptable current ripples due to the IGBT's limited switching frequency. This paper introduces a new multilevel dc link inverter, which can dramatically reduce the current ripple for brushless PM motor drives. The operating principle and design guidelines are included.**

I. Introduction

In permanent magnet (PM) motors, the main flux is produced by the magnets either mounted on the surface of or buried inside the rotor. Because the magnets do not carry current, copper loss is eliminated from the rotor. Further, PM motors can operate at nearly unity power factor. Hence, PM motors have higher efficiency compared to induction motors. Moreover, it is easier to achieve high-performance torque control with PM motors, in particular, brushless direct current (BLDC) motors or brushless PM motors. Owing to these advantages, PM motors have been widely used in a variety of applications in industrial automation and domestic appliances with power levels up to 10 kW[1][2]. Recent advancements in magnetic materials and motor design techniques have made the PM motor an excellent candidate for traction drives in electric/hybrid-electric vehicle applications [3][4].

Due to a long effective air gap, PM motors tend to have low inductance. In [5], the air gap is intentionally made large to reduce the flux harmonics caused by stator slots and thus the resultant iron loss in the stator is significantly decreased for super-high speed PM motors. Recent design techniques on high power PM motors (several tens of kWs) for EV/HEV applications such as the use of ironless stator structure have reduced the inductance even further below 100 μH [6]. These types of very low inductance PM motors can provide fast current control response, which is favorable for most applications. Ironless motors can produce torque linearly related to the stator current because there is no iron to saturate.

On the other hand, the low inductance imposes a stringent current regulation demand for the inverter to produce a motor current with an acceptable level of current ripple, which is typically required to be lower than 5% for many applications. For low power (up to a few kWs) applications, MOSFETs are usually employed because they can efficiently switch at up to 50 kHz, which can handle moderately low inductance (a few hundred μH) motors. As the power level reaches several tens of kWs the preferred switching device is the IGBT, which is typically available in two- or six-pack modules. IGBT modules can only switch at up to 20 kHz [11][12][13], which is not sufficiently high for very low inductance PM motors.

An analysis of current ripple for BLDC motors having very low inductance is conducted in this paper. It shows that as the inductance decreases below 200 μH traditional PWM inverters with the most commonly used IGBT switching devices will produce unacceptable current ripple due to the IGBT's limited switching frequency. This paper introduces a new multilevel dc link inverter (MLDCL) for BLDC motors having very low inductance. The proposed inverter can meet the strict current regulation by modulating the inverter dc link voltage through dc voltage level stepping and PWM control according to the amplitude of the motor back EMF.

II. Analysis of Current Ripple in BLDC Motors

A PM motor can be excited in synchronous mode or brushless dc mode. The latter excitation, whose drive system cost is low, is well suited for PM motors of a trapezoidal back EMF, while the former excitation is usually employed for motors having sinusoidal back EMF. Fig. 1(a) illustrates a typical traditional BLDC motor drive consisting of a three-phase PWM inverter and a PM motor characterized with trapezoidal phase-to-phase back EMFs defined in Fig. 1(b). In the BLDC mode, only two of the three phase stators that present the peak back EMF are excited by properly switching the active switches of the inverter, resulting in ideal motor current waveforms of rectangular shape. There are six combinations of the stator excitation over a fundamental

[*] Prepared by Oak Ridge National Laboratory, managed by UT-Battelle, LLC, for the U.S. Dept. of Energy under contract DE-AC05-00OR22725.

cycle with each combination lasting for a phase period of π/3, as depicted in the same figure. The corresponding two active switches in each period may perform pulse width modulation to regulate the motor current. To reduce current ripple, it is often useful to have one switch doing PWM while keeping the other conducting instead of having the two switching simultaneously. It is also possible to split each of the six phase periods into segments and alternate the switch doing PWM during each segment to improve the current waveform [8] or to prevent the unwanted circulating current which may occur in the inactive phase [9].

Motor current ripple can be analyzed based on an equivalent circuit for a BLDC motor. For such PWM schemes described above, the equivalent circuit for the two active phases is given in Fig. 2(a), where R_m and L_m are the per-phase stator resistance and leakage inductance, respectively [10]. The commutation overlap during mode transition can be ignored for low inductance motors and is therefore not considered in the equivalent circuit. Fig. 2(b) illustrates motor terminal voltage and current of the two active phases.

Ignoring the state coil resistance, current ripple, defined as the peak deviation from the average current as shown in Fig. 2(b), at steady state and continuous conduction mode can be determined by the following equation.

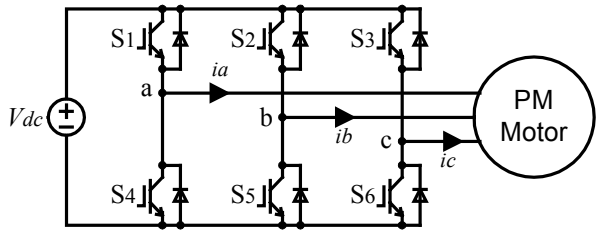

(a) A three-phase BLDC motor drive.

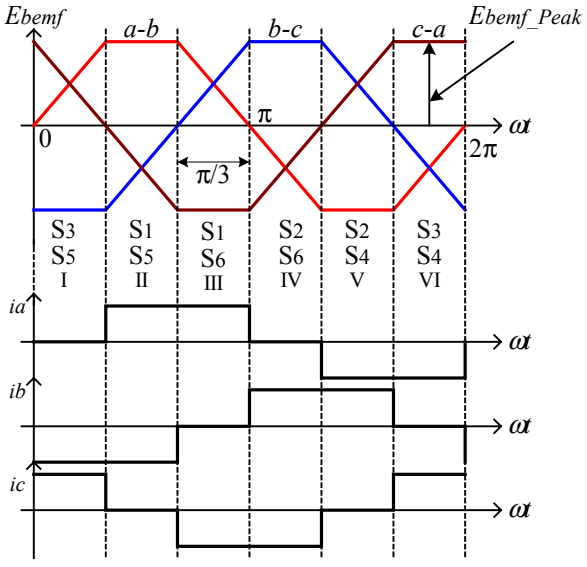

(b) Phase-to-phase back EMFs, ideal motor currents and active switches over an electric cycle for BLDC excitation.

Fig. 1. A traditional PWM inverter for a BLDC motor.

$$I_{m\_ripple} = \frac{1}{4L_m f_{SW}}\left(1 - \frac{E_{bemf\_peak}}{V_{dc}}\right)E_{bemf\_peak} \quad (1)$$

where

f_{SW}: inverter switching frequency, $f_{SW} = 1/Tsw$

V_{dc}: inverter dc link voltage,

E_{bemf_peak}: peak phase-to-phase back EMF.

Assuming the back EMF is linearly related to the motor speed, N by $E_{bemf\_peak} = K_{bemf} N$, where K_{bemf} is a constant determined by the motor, equation (1) can be rewritten as

$$I_{m\_ripple} = \frac{1}{4L_m f_{SW}}\left(1 - \frac{K_{bemf} N}{V_{dc}}\right)K_{bemf} N \,. \quad (2)$$

The maximum current ripple can be determined by

$$I_{m\_ripple(\max)} = \frac{V_{dc}}{16L_m f_{SW}} \quad (3)$$

$$\text{at} \qquad N = \frac{V_{dc}}{2K_{bemf}} \,.$$

The maximum current ripple occurs at the speed at which the back EMF is equal to half the dc bus voltage, and is inversely proportional to the motor inductance and the inverter switching frequency.

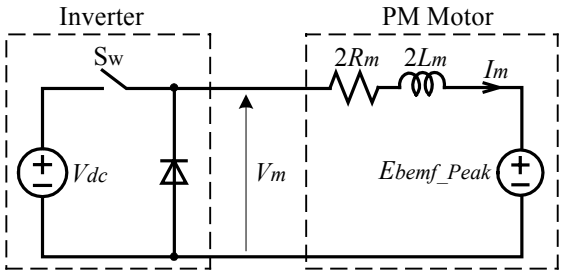

(a) An equivalent circuit for the BLDC motor.

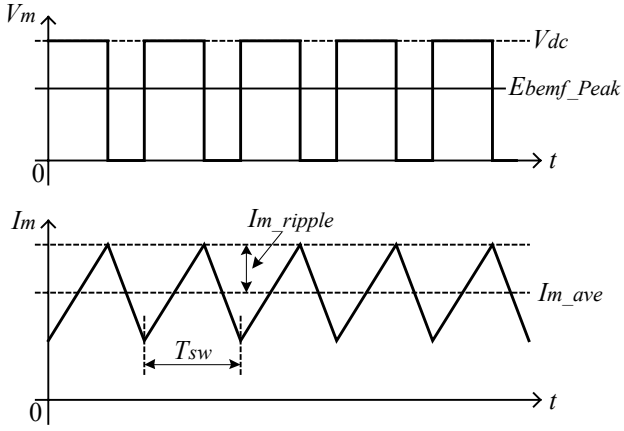

(b) Motor terminal voltage and current waveforms over a phase period of 2π/3 of the two active phases.

Fig. 2. Current ripple analysis for the brushless PM motor.

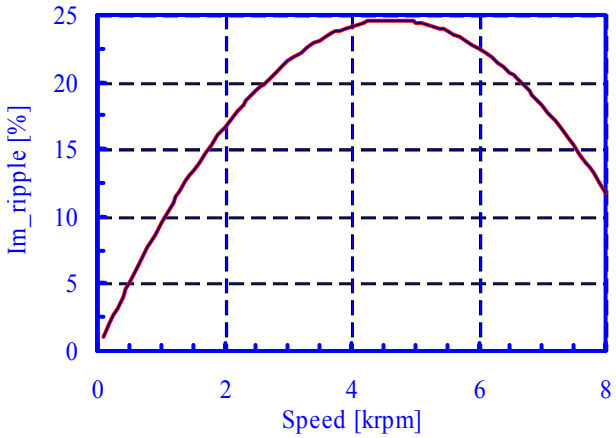

Fig. 3. Current ripple vs. speed for a brussles DC motor having an inductance of 37.5μH (*Vdc*=325V, *fsw*=20kHz).

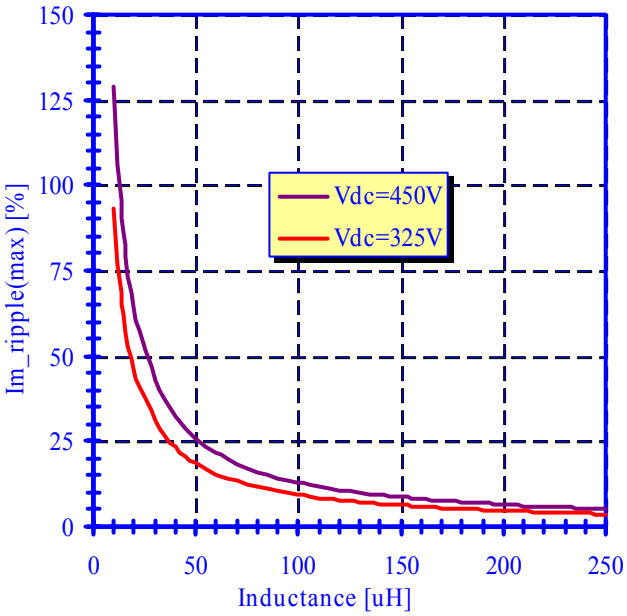

Fig. 4. Maximum current ripple vs. motor inductance for *fsw*=20 kHz.

A plot of current ripple as a percentage of the rated current versus speed is given in Fig. 3 for a 30 kW PM motor having a rated current of 110A and a phase leakage inductance of *Lm*=37.5μH with the inverter switching at 20 kHz and a dc bus voltage of V_{dc}=325V. It shows that a standard inverter with the most commonly used IGBT switching device will produce an unacceptable maximum current ripple of 25% due to the IGBT's limited switching frequency, which must fall below 20 kHz. This high frequency, high current ripple not only causes additional motor losses but also requires that the inverter be overrated to handle the high peak current.

Fig. 4 gives the calculated maximum current ripple as a function of the motor inductance for *fsw*=20 kHz, *Vdc*=450 V and 325 V. In EV/HEV applications, the inverter dc bus voltage is expected to vary widely from 200 V to 450 V with a nominal operating voltage of 325 V. It should also be pointed out that ironless PM motors may have a leakage inductance well below 10 μH. The figure indicates that the maximum current ripple will exceed 5 % as the inductance decreases below 200 μH with the traditional PWM inverters employing IGBT switching devices.

For a given switching frequency, one can reduce the current ripple by adding external inductors to increase the inductance and/or modulating the dc link voltage. Because inductors rated for high current are bulky and a large inductance undesirably slows current control response, the remaining way to reduce current ripple is to modulate the dc link voltage according to the level of back EMF. Although a step-down chopper may be used to regulate the dc voltage, it requires an additional inductor.

The following section introduces a multilevel dc link inverter for PM motors having very low inductance. The proposed inverter can meet the strict current regulation by modulating the inverter dc link voltage through dc voltage level stepping and PWM control depending on the amplitude of the back EMF.

III. Proposed Multilevel Inverter

A. Multilevel DC Link Inverter Topology

Fig. 5 shows the proposed inverter topology supplying a PM motor, which consists of a multilevel dc source and a standard bridge inverter. The dc source is formed by connecting a number of cells in series with each cell having a voltage source controlled by two switches. The two switches, *Sa* and *Sb* operate in a toggle fashion. The cell source is bypassed with Sa on and *Sb* off or adds to the dc bus voltage by reversing the switches. It is noticed that the source level of each cell is not necessarily required to be equal. In fact, to produce the same number of voltage levels the number of cells can be reduced by properly choosing the voltage source for each cell as discussed in [14].

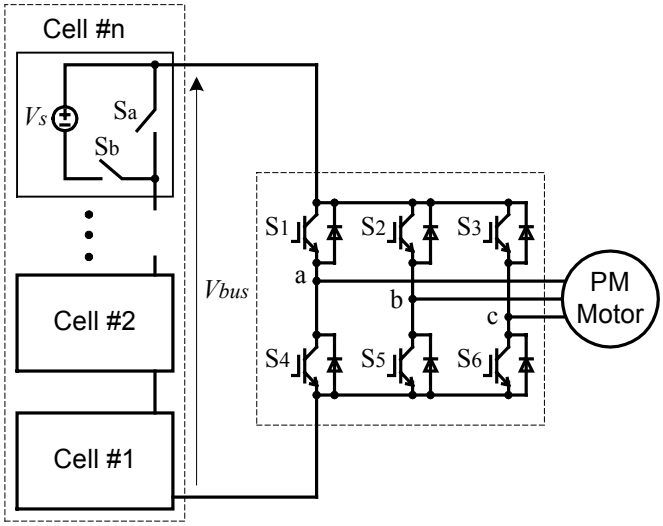

Fig. 5. Proposed n-level MLDC link inverter for BLDC motor drive.

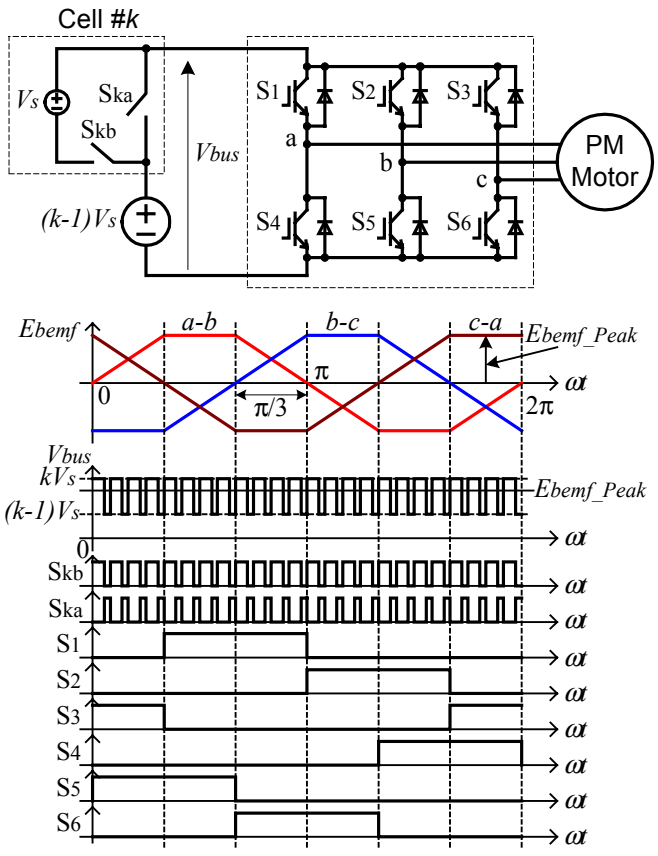

Fig. 6. Operating principle.

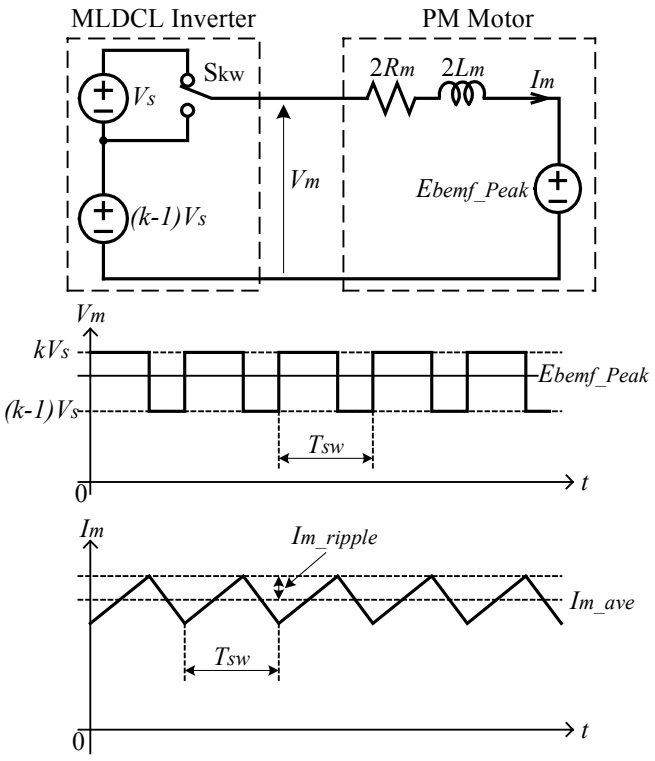

Fig. 7. An equivalent circuit and operating waveforms.

B. Operating Principle

Fig. 6 illustrates the operating principle. To control a PM motor in BLDC mode, the bridge inverter is used only to commutate the motor phase currents without doing PWM for current regulation. The current regulation is accomplished by the switches in the cells. For a given range of back EMF defined by its minimum $E_{bemf\_Peak(\min)}$ and maximum $E_{bemf\_Peak(\max)}$, a portion of the cells are active but only one of the cells performs PWM while the rest of the active cells always add to the dc bus, as shown in Fig. 6. The sources of the inactive cells are bypassed. This is important to keep the current ripple down because the current ripple is proportional to the differences between the dc bus voltage and back EMF during the current rising period and the subsequent falling period over each switching cycle. The required number of active cells, k, is determined by

$$\frac{E_{bemf\_Peak(\max)}}{V_s} < k < \frac{E_{bemf\_Peak(\min)}}{V_s} + 1 \quad (4)$$

where Vs is the source voltage of each cell. Since n cells cover the full voltage range, it is obvious that $1<=k<=n$ and that the number of active cells increases with motor speed. It is also useful to rotate the active cells and the cell performing PWM so that the same amount of average power is drawn from each cell source [15].

Alternatively, for a given number of cells, the controllable speed range is defined by

$$\frac{(k-1)V_s}{K_{bemf}} < N < \frac{kV_s}{K_{bemf}} \quad . \quad (5)$$

C. Current Ripple Analysis

The current ripple at steady state and continuous conduction mode can be derived from the equivalent circuit and the operating waveforms shown in Fig. 7 as follows.

$$I_{m\_ripple} = \frac{k^2 V_s}{4 L_m f_{SW}} \left(1 - \frac{K_{bemf} N}{k V_s}\right)\left(\frac{K_{bemf} N}{k V_s} - \frac{k-1}{k}\right) \quad (6)$$

The maximum current ripple can be determined by

$$I_{m\_ripple(\max)} = \frac{V_s}{16 L_m f_{SW}} \quad \text{at} \quad N = \frac{(2k-1)V_s}{2K_{bemf}} \quad . \quad (7)$$

From equations (3) and (7), the maximum current ripple is reduced by a factor of V_{dc}/V_s, i.e. the number of cells. It is worth noting that the motor terminal voltage Vm swings between $(k-1)Vs$ and kVs in the MLDCL inverter (Fig. 7) while it swings between 0 and the full bus voltage Vdc in the traditional PWM inverter (Fig. 2). Hence dv/dt can also be reduced significantly with the MLDCL inverter.

Fig. 8 gives the required number of voltage levels as a function of the motor leakage inductance to keep the maximum current ripple below 5 % for a maximum dc bus voltage of 450 V and 325 V with the cell switches operating at 20 kHz. Fig. 9 shows the corresponding maximum current ripple.

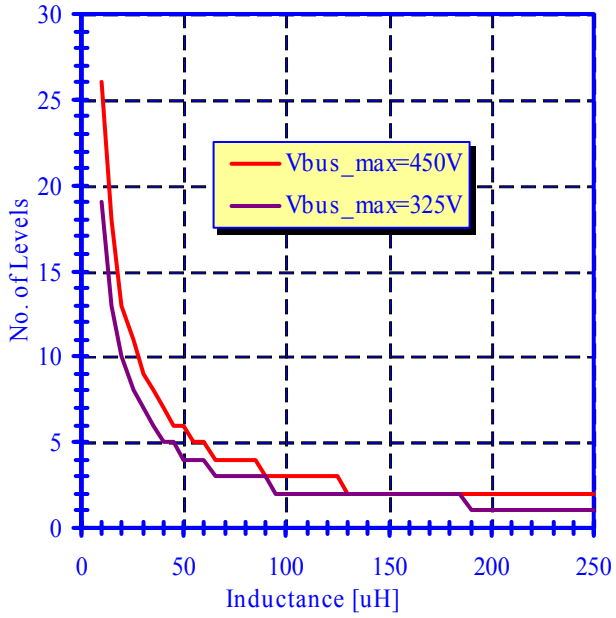

Fig. 8. Required number of levels for keeping the maximum current ripple below 5% with *fsw*=20kHz.

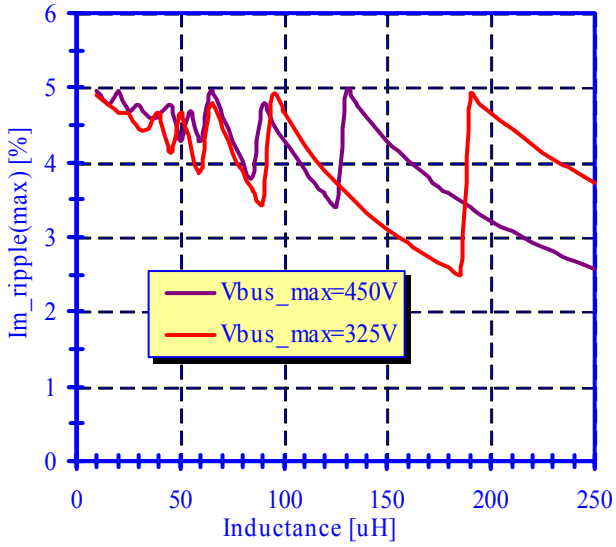

Fig. 9. Maximum current ripple for the selected number of levels in Fig. 8 at *fsw*=20kHz.

D. Design Example

Given the maximum bus voltage of 325 V for the same PM motor described in section II, the required number of voltage levels is 5 to keep the current ripple below 5 %. The voltage source of each cell, *Vs*, is thus 65 V. Fig. 10(a) shows a five-level inverter, which employs power MOSFETs as the cell switches since the cell voltage is low. The use of MOSFETS provides an additional option for further ripple reduction and that is to switch at frequency higher than 20 kHz. Fig. 10(b) plots the calculated current ripple with the MLDCL inverter. For comparison, the current ripple with the traditional inverter is also plotted. The maximum current ripple is reduced by a factor of 5 as expected.

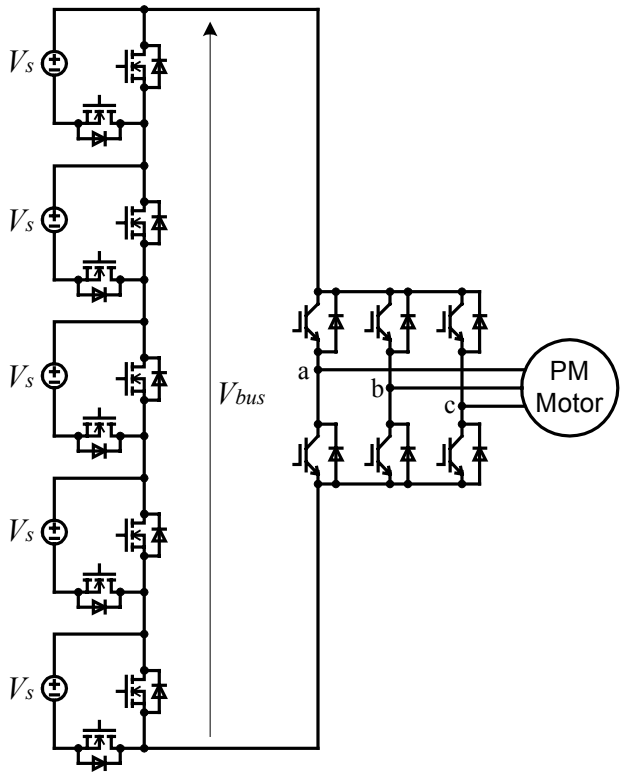

(a) A five level dc link inverter using MOSFETs as cell switches.

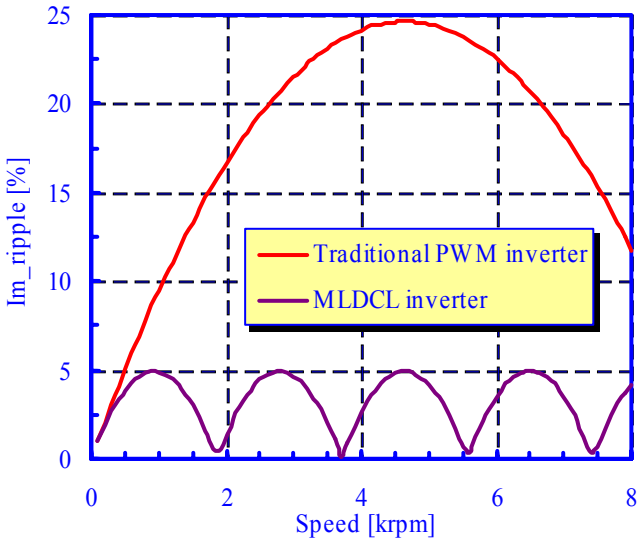

(b) Calculated motor current ripple.

Fig. 10. A 5 level dc link inverter for BLPM motor drive. Cell Voltage (*Vs*): 65V, motor inductance (*Lm*): 37.5 µH, *fsw*=20kHz.

IV. Simulation Results

Detailed circuit simulation verified the analysis. Fig. 11 shows a comparison of motor current waveforms between the traditional inverter and the proposed MLDCL inverter, where both inverters are switching at 20 kHz. It shows a clear reduction in the current ripple with the proposed inverter, confirming the analysis. It should be noted that all cells are utilized during mode transition, as can be seen from the dc bus voltage waveform, *Vbus*, in (b) to help building-up the incoming phase current, thus reducing the commutation notches in the current.

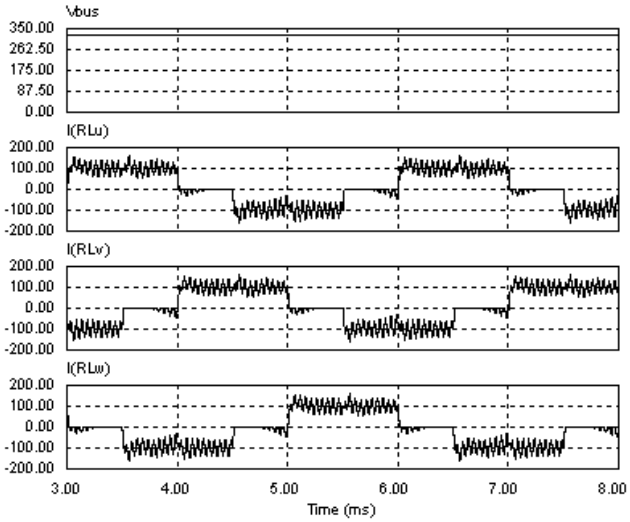

(a) With a traditional PWM Inverter.

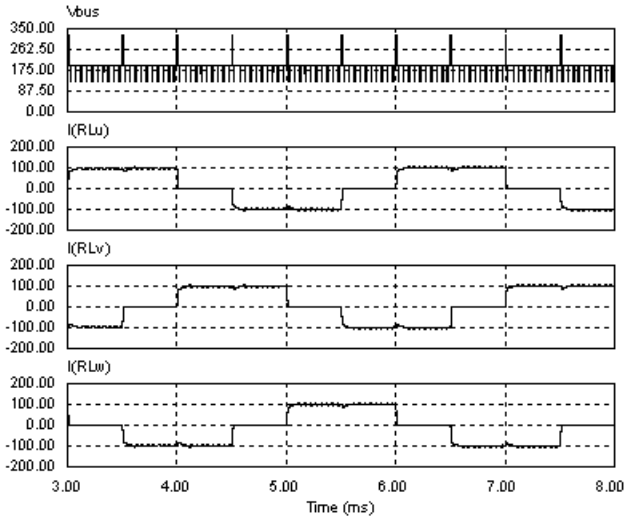

(b) With the 5 level MLDCLI PWM Inverter.

Fig. 11. Comparison of simulated motor current waveforms at 5000 rpm.

V. Conclusions

This paper introduces a new multilevel dc link inverter topology for very low inductance PM motors operating in brushless dc mode. Useful design equations are included. The analysis and simulation results show that the proposed inverter can dramatically reduce current and thus torque ripples. Consequently, motor efficiency can be improved because of the reduced copper and iron losses as a result of the reduced current ripple.

The proposed MLDCL inverter can also be applied for switched reluctance motor drives.

It is noted that other multilevel configurations such as the diode clamped multilevel inverter can also be adapted for the proposed topology, but they introduce a charge balance difficulty among the cells.

Acknowledgment

The authors thank Drs. John McKeever and Leon Tolbert for their proof reading and insightful discussions.

References

[1] D. M. Erdman, H. B. Harms, J.L. Oldenkamp, "Electronically Commutated DC Motors for the Appliance Industry," Conf. Rec. 1984 IEEE Ind. Applicat. Soc. Ann. Mtg., pp. 1339-1345.

[2] B. V. Murty, "Fast Response Reversible Brushless DC Drive with Regenerative Breaking," Conf. Rec. 1984 IEEE Ind. Applicat. Soc. Ann. Mtg., pp. 445-450.

[3] C. C. Chen et al, "A novel polyphase multipole square-wave permanent magnet motor drive for electric vehicles", *IEEE Trans. Ind. Applicat.*, vol. IA-30, pp. 1258-1266, Sep./Oct. 1994.

[4] F. Caricchi, F. Crescimbini, F. Mezzetti, E. Santini, "Multistage axial-flux PM machine for wheel direct drive," *IEEE Trans.Ind. Applicat.*, vol. 32, no. 4, pp. 882 –888, July-Aug. 1996.

[5] I. Takahashi, et al "A Super High Speed PM Motor Drive System by a Quasi-Current Source Inverter", *IEEE Trans. Ind. Applicat.*, vol. 30, pp. 683-690, May/June 1994.

[6] F. Caricchi, et al "Performance of Coreless-Winding Axial-Flux Permanent-Magnet Generator with Power Output at 400 Hz, 3000 r/min", *IEEE Trans.Ind. Applicat.*, vol. 34, pp. 1263-1269, Nov./Dec. 1998.

[7] J.-O. Krah and J. Holtz, "High Performance Current Regulation and Efficient PWM Implementation for Low-Inductance Serveo Motors", *IEEE Trans. Ind. Applicat.*, vol. 35, pp. 1039-1049, Sept./Oct. 1999.

[8] G.J. Su, J. Mckeever and K. Samons, "Design of a PM Brushless Motor Drive for Hybrid Electric Vehicle Application," PCIM 2000, Boston, MA, pp. 35-43, 2000.

[9] C. Namuduri and K. Gokhale, "Pulse Width Modulation Control Apparatus and Method," U.S. Patent 5,264,775, Nov., 1993.

[10] P. Pillay and R. Krishnan, "Modeling, Simulation, and Analysis of Permanent-Magnet Motor Drives, Part II: The Brushless DC Motor Drive", *IEEE Trans. Ind. Applicat.*, vol. 25, pp. 274-279, Mach/April 1989.

[11] "IGBTMOD and Intellimod™ – Intelligent Power Modules Applications and Technical Data Book", Powerex, 2000.

[12] "Fuji Electric R Series Intelligent Power Module Specifications", Collmer Semiconductor, INC, 1999.

[13] Semikron CD-ROM Data Book, 2000.

[14] M. D. Manjrekar and T. A. Lipo, "A hybrid multilevel inverter topology for drive applications," Proc. IEEE APEC'98, pp. 523-529, 1998.

[15] F. Z. Peng, J. W. McKeever and D. J. Adams, "A power line conditioner using cascade multilevel inverters for distribution systems," *IEEE Trans. Ind. Applicat.*, vol. 34, pp. 1293 -1298, Nov./Dec., 1998.